OPEN ACCESS

University of BRISTOL

Balasubramanian, M., Padidela, R., Pollitt, R. C., Bishop, N. J., Mughal, M. Z., Offiah, A. C., ... Stephens, D. J. (2017). P4HB recurrent missense mutation causing Cole-Carpenter syndrome. *Journal of Medical Genetics*. https://doi.org/10.1136/jmedgenet-2017-104899

Peer reviewed version

Link to published version (if available):
10.1136/jmedgenet-2017-104899

Link to publication record in Explore Bristol Research
PDF-document

This is the author accepted manuscript (AAM). The final published version (version of record) is available online via BMJ at http://jmg.bmj.com/content/early/2017/12/19/jmedgenet-2017-104899. Please refer to any applicable terms of use of the publisher.

University of Bristol - Explore Bristol Research

General rights

This document is made available in accordance with publisher policies. Please cite only the published version using the reference above. Full terms of use are available:
http://www.bristol.ac.uk/pure/about/ebr-terms

P4HB recurrent missense mutation causing Cole-Carpenter syndrome

Running Title: *P4HB* causing severe CCS

Meena Balasubramanian[1,2], Raja Padidela[3], Rebecca C Pollitt[4,5], Nicholas J Bishop[4], M Zulf Mughal[3], Amaka C Offiah[4], Bart E Wagner[6], Janine McCaughey[7], David J Stephens[7]

[1]Sheffield Clinical Genetics Service, Sheffield Children's NHS Foundation Trust, UK

[2]Highly Specialised Service for Severe, Complex and Atypical OI Service, Sheffield Children's NHS Foundation Trust, Sheffield, UK

[3]Department of Paediatric Endocrinology, Royal Manchester Children's Hospital, Central Manchester University Hospitals NHS Foundation Trust, UK

[4]Academic Unit of Child Health, University of Sheffield, UK

[5]Sheffield Diagnostic Genetics Service, Sheffield Children's NHS Foundation Trust, UK

[6]Department of Histopathology, Royal Hallamshire Hospital, Sheffield, UK

[7]School of Biochemistry, University of Bristol, Bristol, UK

Correspondence to:

Dr Meena Balasubramanian

Sheffield Clinical Genetics Service

Sheffield Children's NHS Foundation Trust

Western Bank, Sheffield S10 2TH

Ph- +44 114 2717025; Fax- +44 114 2737467

E-mail-meena.balasubramanian@sch.nhs.uk

Keywords: osteogenesis imperfecta, *P4HB*, collagen processing, recurrent mutation, skeletal dysplasia

ABSTRACT

Background: Cole-Carpenter syndrome (CCS) is commonly classified as a rare Osteogenesis Imperfecta (OI) disorder. This was following the description of two unrelated patients with very similar phenotypes who were subsequently shown to have a heterozygous missense mutation in *P4HB*.

Objective(s): Here, we report a 3-year old female patient with severe OI who on exome sequencing was found to carry the same missense mutation in *P4HB* as reported in the original cohort. We discuss the genetic heterogeneity of CCS and underlying mechanism of *P4HB* in collagen production.

Methods: We undertook detailed clinical, radiological and molecular phenotyping in addition, to analysis of collagen in cultured fibroblasts and electron microscopic examination in the patient reported here.

Results: The clinical phenotype appears consistent in patients reported so far but interestingly, there also appears to be a definitive phenotypic clue (crumpling metadiaphyseal fractures of the long tubular bones with metaphyseal sclerosis which are findings that are uncommon in OI) to the underlying genotype (*P4HB* variant).

Discussion: *P4HB* (Prolyl 4-hydroxylase, beta subunit) encodes for PDI (Protein Disulfide isomerase) and in cells, in its tetrameric form, catalyses formation of 4-hydroxyproline in collagen. The recurrent variant in *P4HB*, c.1178A>G, p.Tyr393Cys, sits in the C-terminal reactive centre and is said to interfere with disulphide isomerase function of the C-terminal reactive centre. P4HB catalyses the hydroxylation of proline residues within the X-Pro-Gly repeats in the procollagen helical domain. Given the inter-dependence of extracellular matrix (ECM) components in assembly of a functional matrix, our data suggest that it is the

organisation and assembly of the functional ECM that is perturbed rather than the secretion of collagen type I per se.

Conclusions: We provide additional evidence of P4HB as a cause of a specific form of OI-CCS and expand on response to treatment with bisphosphonates in this rare disorder.

INTRODUCTION

In 1987, Cole and Carpenter reported two unrelated infants with multiple fractures and deformities of bone, with a skeletal phenotype similar to severe osteogenesis imperfecta (OI). In addition, these patients also had proptosis, blue sclerae, hydrocephalus and a distinct facial gestalt. They were reported to be of normal intelligence.[1] Radiologically, these patients had characteristic skeletal manifestations including craniosynostosis, in addition to the deformities seen in severe progressive OI.

Since the first description, there was only one further report of a patient with a similar phenotype [2] until Balasubramanian et al., 2015 described a 12-year old patient with phenotypic Cole-Carpenter syndrome (CCS) who had homozygous mutations in *CRTAP* and described CCS as a variant of recessive OI.[3] This patient had the characteristic facial features, ocular proptosis, craniosynostosis (corrected in childhood) and severe bone fragility (needing treatment with bisphosphonates). In 2015, two reports were published describing the aetiology of CCS[4,5]: Rauch *et al*., described a heterozygous missense mutation in *P4HB* in the original cohort of patients; this came to be known as Cole-Carpenter syndrome 1 (CLCRP1 OMIM #11240). Garbes *et al*., 2015 reported a German boy with phenotypic Cole-Carpenter syndrome and 2 fetuses from terminated pregnancies with antenatal presentation of a severe bone fragility in a separate German family. All patients in this cohort were found to have compound heterozygous mutations in *SEC24D*. The authors described their presentation

to be overlapping with Cranio-lenticulo-sutural dysplasia (CLSD OMIM #607812) caused by mutations in a related COPII gene, *SEC23A* but summarised the phenotype to be more like CCS. This has now come to be known as Cole-Carpenter syndrome 2 (CLCRP2 OMIM #616294). Table 1 provides an overview of the clinical, radiological and molecular diagnosis of patients with CCS reported in the literature and this patient.

Therefore, it appears that CCS is a genetically heterogeneous condition with a strikingly similar phenotype, common features being severe bone fragility and distinct facial dysmorphism with/ without craniosynostosis. The facial dysmorphism mainly comprises relative macrocephaly with wide open fontanelle, blue sclera, small nose, flat nasal bridge, a broad face with ocular proptosis. This is perhaps slightly different to the facial features characteristically seen in OI due to other genetic aetiology.

Here we describe a 3-year old patient with severe bone fragility, who on exome sequencing, was shown to have the same missense mutation as described by Rauch et al., 2015. Reverse phenotyping suggested that this patient was likely to be in the CCS spectrum and functional studies were undertaken in hpf (human primary fibroblasts).

CLINICAL REPORT

The proband is the first child of healthy, non-consanguineous White, European parents with no significant family history. She has an older maternal half-brother who is fit and well. The pregnancy was unremarkable with no suggestions antenatally of bone fragility. She was born in a good condition at term with a birth weight of 3710 grams (z score 0.6). From one week of age, her oral intake reduced and she was noted to be irritable. She had multiple admissions for suspected urinary tract infection, however, her ultrasound scans of the renal tract, micturating cystourethrogram and DMSA scan were all normal. She was diagnosed with

positional talipes for which she received physiotherapy. At 6 months of age, she presented with a left distal tibial fracture. On clinical examination, she was noted to have failure to thrive (weight Z score reduced to -1.4), relatively large head with wide open fontanelle, blue sclera, small nose, flat nasal bridge, right upturned ear lobe, a broad face, long fingers, relatively broad thumbs and great toes (Figure 1a-c). A skeletal survey showed diffusely osteopenic bones with multiple vertebral body compression fractures in the thoracic and lumbar spine and fractures of the anterior left 8^{th}, 9^{th} and 10^{th} ribs. She had Wormian bones over sagittal and lambdoid sutures noted on her skull radiograph and old fractures of both distal radial shafts. All long bones showed "crumpling" metaphyseal fractures with widening, sclerosis, and irregularity of the distal metaphyses (Figure 2a-e).

A clinical diagnosis of osteogenesis imperfecta (OI) was made and she was commenced on intravenous bisphosphonate (pamidronate) infusions from 7 months of age, which she continues to receive at the current age of 3 years and 8 months. Until 2 years and 8 months of age, she had multiple non-traumatic fractures of long bones of her upper and lower limbs. Her vertebral fractures have, however, significantly improved with remodelling of all vertebral bodies. She had corrective tibial osteotomies and bilateral tibial rodding's with Fassier–Duval lengthening rods at 2 years and 8 months of age and she is currently awaiting the surgical correction of deformities of her both femora and upper limb bones. Developmentally, she has progressed well with her speech and language and social skills. Her gross motor development has been delayed because of her limb bone deformities.

At a recent Genetics review at 3-years of age, she was noted to be in a mainstream nursery and had not sustained any fractures in the last 18 months. She was wearing glasses for a squint and her teeth were noted to be brittle but with no evidence of dentinogenesis imperfecta. Her growth parameters were, weight 12.5 kilograms (Z score -1.84), height 77 cms (Z score -4.99) and head circumference 54 cms (Z score +2.5); she was noted to have

frontal bossing with a broad face, flat nasal bridge, prominent eyes with bilateral low-set ears (Figure 1d) and bilateral limb deformities.

Genetic testing prior to whole exome sequencing included targeted OI panel testing which at that time included all genes so far published in dominant and recessive OI (October 2014); dosage analysis of *COL1A1/A2* genes using MLPA which was reported negative. She was subsequently recruited to a research study being undertaken in children with atypical OI with appropriate parental consent.

MATERIALS AND METHODS

This patient was recruited into a research project to study atypical forms of OI, to establish genotype: phenotype correlations. Funding was obtained from the Children's Hospital Charity and ethical approval was obtained from the local regional ethics committee (REC reference: 15/YH/0362) to undertake phenotyping and genetic work-up in this group of patients.

DNA sequencing and exome sequencing:

Whole exome sequencing was performed using SureSelect QXT library preparation method and SureSelect Human All Exon V6 baits for target enrichment. Libraries were sequenced on a HiSeq 2500 using paired-end sequencing 2x100bp. Bcl2fastq (v1.8.4) was used to convert sequencing data to fastq files. Fastq files were uploaded to Sapienta (v1.5.0) for mapping and variant calling. Sapienta does not provide a whole exome coverage summary; however, after mapping with bwa mem (0.7.15) to GRCh37, a mean exonic coverage of 103x (standard deviation 62.1) and a median of 94x was obtained. Bases contribute to coverage if their quality is >= 30 and mapping quality is at least 10 for the read within which they are

contained. Duplicate reads are excluded. "SureSelect Human All Exon V6 r2" design files were used to restrict coverage calculations; here we state values for the "Covered" bed file.

Variants reported with a frequency > 1% in the NHLBI ESP or ExAC cohort populations were excluded. Further filtering of variants to look for potential loss of function changes (frameshift, splice site acceptor, splice site donor, or stop gained) was undertaken. Finally, a larger group of variants within a targeted gene list was assessed. The gene list consisted of those reported in connection with bone dysplasias, identified in GWAS studies of change in bone density, implicated in bone metabolism in mouse models, and genes with human phenotype ontology terms relating to increased susceptibility to fracture, totalling approximately 600 genes.

Electron Microscopy from skin biopsy

Electron microscopy (EM) of the skin ellipse biopsy specimen was performed by: fixing in 3% phosphate buffered glutaraldehyde, post-fixation in 2% aqueous osmium tetroxide, processing to epoxy resin and at embedding, orientation to display sections of epidermis and full thickness dermis. Toluidine blue stained semi-thin sections (0.6um) were assessed by light microscopy, and thin sections (85nm) were cut on an ultramicrotome using a diamond knife, mounted on a 200 thin bar hexagonal mesh copper grid. The material was stained with uranyl acetate and lead citrate and 7 grid meshes were examined using a Philips 400 transmission EM. Image capture and collagen fibril diameter quantitations were performed using an AMT 16 megapixel mid mount digital camera. The diameters of 301 unselected collagen fibrils, sectioned transversely, from 5 collagen bundles, at original magnification x20.000, in the mid reticular dermis, were measured. The diameters of 318 collagen bundles were measured, at original magnification x550. The mean of the mean diameters, range, and deviation root mean squared (RMS) were calculated. In addition, collagen fibrils were

checked for the presence of collagen flowers, and fibroblasts were examined for expanded rER, and elastic fibres for structural abnormalities.

Collagen analysis on cultured fibroblasts

Primary patient-derived fibroblasts were cultured in Ham's F10 supplemented with 12% fetal calf serum. Cells were grown for 72 hours on glass coverslips and incubated in the presence of 167 µM (50µg per ml) ascorbic acid for 0.5 or 24 hours, respectively, prior to fixation. Cells were fixed with 4% paraformaldehyde in PBS and processed for immunofluorescence using anti-collagen IαI (Novus Biologicals NB600-408) and imaged by confocal microscopy as described previously using an Alexa-Fluor-568-conjugated secondary antibody (Thermo Fisher Scientific), Prolong Diamond with DAPI for mounting and a Leica SP5 for analysis and image acquisition.[6] Images were compared using automated segmentation of collagen fluorescence intensity using Volocity (version 6.3, Perkin Elmer). Statistical analysis was performed using an unpaired Student's t-Test (p-values).

For semi-quantitative analysis of COL1a1 levels in control and patient cells, cells were seeded confluent and grown for 24 hours. Subsequently, cells were incubated in serum free Ham's F10 medium supplemented with or without 167 µM (50µg per ml) ascorbic acid for 24 hours. The medium was collected, and the cells lysed for 15 minutes in buffer containing 50mM Tris-HCl, 150mM NaCl, 1% (v/v) triton-X-100, 1% (v/v) protease inhibitor cocktail (Calbiochem) at pH 7.4 on ice. Protein fractions of medium and lysate were centrifuged at 13500 rpm at 4 °C for 10 min. The cell pellet was discarded. The supernatant was denatured and run under reducing conditions on a 7% Tris-Acetate precast gel (NuPAGE ®) for 135 min at 100V in Tris-Acetate running buffer supplemented with antioxidant. Transfer of protein bands onto a nitrocellulose membrane was performed at 15 V overnight. The membrane was blocked using 5% (w/v) milk powder in TBST for 30 minutes at RT and

incubated with antibodies against collagen IαI (Novus Biologicals NB600-408; rabbit, 1:500) and GAPDH (Thermo Fisher Scientific AM4300, mouse, 3:1000) as loading control for 1.5 hours at RT. After repeated rinsing with TBST, the membrane was incubated for 1.5 hours at RT with HRP-conjugated antibodies diluted in the blocking solution (1:5000) against mouse and rabbit, respectively. The wash step was repeated, and detection was performed using Promega WB-ECL reaction reagents and autoradiography films with overnight exposure and subsequent development.

RESULTS

Genetic analysis:

Exome sequencing identified a heterozygous c.1178A>G, p.Tyr393Cys pathogenic mutation in exon 9 of *P4HB* (NM_000918.3) (Figure 3). This mutation is predicted to replace tyrosine at position 393 with a cysteine; *in silico* analysis supports its likely pathogenicity. This result was confirmed by Sanger sequencing. DNA was only available from the mother and she tested negative for this mutation; the father's sample was not available for analysis.

Electron microscopy:

Patient elastic tissue and fibroblasts were unremarkable with no collagen flowers seen (Figure 4a). The mean collagen fibril diameter was 74nm, with a range from 39 to 95nm (RMS deviation 7 to 10nm) with a mean collagen bundle diameter of 3.3µ. These parameters were within the normal range for patient age. Adjacent to the sweat gland tubules, there were areas of small collections of individual collagen fibrils with proteoglycans wrapping around them (Figure 4b), the significance of which is uncertain.

Collagen analysis:

Collagen deposited by patient fibroblasts in culture showed not statistically detectable differences (with a p-value of 0.76 for the quantified mid-intensity and 0.34 for high-intensity deposition) compared to controls (Figure 5). While there was a slight trend towards a steady-state decrease in collagen secretion, at short times of incubation in the presence of ascorbic acid, we detected no differences in gross organisation or secretion of type 1 collagen.

DISCUSSION

P4HB (Prolyl 4-hydroxylase, beta subunit), also known as 'Procollagen-proline 2-oxoglutarate-4-dioxygenase, beta subunit (OMIM *176790) maps to chromosome 17q25.3 and spans 18Kb with 10 exons (Pajunen et al., 1991). *P4HB* encodes for PDI (Protein Disulfide isomerase) and in nucleated cells, in its tetrameric form, assists in the formation of 4-hydroxyproline in collagen by P4HA prolyl hydroxylase. It is likely that the recurrent missense mutation in *P4HB* results in a very specific form of bone fragility by interfering with collagen formation, which could conceivably be associated with additional changes in deposition and/or assembly of extracellular matrix (ECM).

Cole-Carpenter syndrome [OMIM 112240] is mainly characterised by bone fragility, craniosynostosis, ocular proptosis, hydrocephalus and a distinctive facial appearance. Intelligence is reported to be normal. In their original report, Cole and Carpenter described two patients[(1)]: Patient 1 had multiple fractures, frontal bossing, proptotic appearance and progressive hydrocephalus. Skeletal survey at 4-months of age showed numerous metaphyseal irregularities and compression fractures in the long bones. Progressive craniosynostosis was noted at 9-months of age. His voice was noted to be high-pitched, but words were reported to be well-formed. Patient 2 had hypotonia and failure-to-thrive noted at 2-months of age and facial dysmorphism was noted including micrognathia, frontal

bossing and proptotic appearance. A skeletal survey showed multiple metaphyseal compression fractures. In the report, the authors concluded that both patients had a variant form of osteogenesis imperfecta, but with additional findings of multiple metaphyseal irregularities, craniosynostosis, hydrocephalus, ocular proptosis and a distinctive face that was not characteristic of any known syndromes with craniosynostosis or type of OI. Both patients were reported to have normal neurological development (when reported Patient 1 was 4 years and Patient 2 was 19 months of age).

Rauch et al., 2015 described re-evaluation of these children as adults and reported both Patient 1 and 2 as using a wheelchair with severe scoliosis and marked limb deformities; treatment with intravenous pamidronate over the previous 12-months in Patient 1 and over 3 years in Patient 2 had not altered their clinical status.[(4)] The radiographs in that paper clearly show the additional effects of prolonged immobility in association with the severe bone disease, notably gracile long bones with popcorn epiphyses. WES on genomic DNA was performed on both patients which revealed the same heterozygous variant c.1178A>G, p.Tyr393Cys in exon 9 of *P4HB*. The mechanism pertaining to gain-of-function of mutant PDI protein was proposed and tested which has not been replicated in the current study.

In this report, we identified the same missense mutation in another patient with severe OI who has clinical overlap with CCS and how this variant results in severe bone fragility. The obvious difference in our patient clinically is the age at which pamidronate was commenced (7-months) which appears to have ameliorated the phenotype with reduced fracture frequency, vertebral fracture incidence and reduced distress which she suffered in the first few months of life. This may be supportive of early benefits of commencing treatment in patients with CCS.

The clinical phenotype appears consistent in patients reported so far with CCS but interestingly, there also appears to be an emerging, distinctive radiological phenotype with what appears to be a definitive phenotypic clue to the underlying genotype (*P4HB* mutation). Figure 2 demonstrates metadiaphyseal 'crumpling' fractures with metaphyseal sclerosis in the long tubular bones, findings that are uncommon in OI and may be a pointer to the role in disease of this specific mutation. Patient 1 described by Cole and Carpenter also has the same metadiaphyseal compression fractures with irregular sclerosis and lucencies and subsequent bowing deformity (Figure 1 in Cole and Carpenter paper). Therefore, we propose that the metaphyseal 'crumpling' fractures with metaphyseal sclerosis may be a clue to the underlying genotype. This was dissimilar to the findings of osteopenia and bowing with fractures in radiographs of patient reported by Amor et al., 2000 who did not share similar radiological findings as described above and tested negative for the *P4HB* recurrent mutation.[(2)] Interestingly, reviewing the radiographs of the patient reported by Balasubramanian et al., 2015 with phenotypic CCS who has homozygous variants in *CRTAP*, the metaphyseal compression fractures and sclerosis were not present, thus adding further evidence to this observation.[(3)]

P4HB encodes the beta subunit of prolyl 4-hydroxylase which is a highly abundant multi-functional enzyme belonging to the protein disulphide isomerase (PDI) family. The PDI family comprises PDI and PDI-like proteins with more than twenty members having been studied in humans.[(7)] PDI is usually found in the endoplasmic reticulum (ER) but can also be released to function at the extracellular matrix or cell surface. PDI is the most abundant family member comprising 0.8% of total cellular protein in yeast and mammalian cells [(8)] and is critical for cell viability in yeast.[(9)] It functions as a redox catalyst and as a chaperone by preventing protein aggregation in the ER or by retaining proteins within the ER where necessary.[(10)]

P4HB comprises four TRX-like (thioredoxin-like) domains termed a, b, b', a', a linker (x) and a C-terminal extension domain organised in the order of abb'xa'c. However, only two of these four domains (a and a') have disulphide isomerase activity and are separated from each other by the enzymatically inactive b and b' domains. P4H exists as a 2:2 stoichiometric heterotetramer and is generally called the α-subunit existing as three isoforms (α (I), α (II) and α (III). All three α subunits require a β-subunit i.e. PDI to form an enzymatically active complex. The PDI β-subunit is required to maintain the solubility of the P4H α subunit and keep the complex within the ER. As well as the disulphide isomerase activity, the tetrameric form is active in hydroxylation of proline residues within preprocollagen. Therefore, PDI as a stand-alone disulphide isomerase and as a P4H heterotetramer, is crucial for procollagen biosynthesis.[11]

Hence, PDI family members function as molecular chaperones and as disulphide oxidoreductase/isomerases. As a result, they can make, break or rearrange disulphide bonds in client proteins, including collagen and extracellular matrix proteins. These disulphide bonds are essential to ensure the protein has structural stability and also to keep multimeric complexes together. Cellular function relies on the ability of proteins to adopt their correct folds and it is very well recognised that misfolded proteins are known to result in disease; this is especially true in OI. However, it should be noted that the recurrent *P4HB* mutation reported here does not directly alter the catalytic CGHC motif of PDI. Rather, the mutation results in the gain of a cysteine residue, which may lead to a "gain of function" phenotype. In this scenario, PDI could either misoxidise, fail to interact appropriately with P4HA or interact inappropriately with other proteins through spurious inter-molecular disulphide bonds.

The recurrent mutation in *P4HB*, c.1178A>G, p.Tyr393Cys, sits towards the C-terminus and is said to interfere with disulphide isomerase function. P4HB catalyses the hydroxylation of proline residues within the X-Pro-Gly repeats in the procollagen helical domain. However,

our data indicates no major difference in extracellular collagen type I deposition by patient fibroblasts, as judged by immunofluorescence. While there was a minor trend towards an increase in extracellular collagen type I compared to the control, this was not statistically significant. Our experiments do not define whether this collagen is triple helical and we have not examined other collagen types or proteoglycans. Given the inter-dependence of ECM components in assembly of a functional matrix, our data suggest that it is possible that it is the organisation and assembly of the functional ECM that is perturbed rather than the secretion of collagen type I *per se*. We postulate that the defect might arise from overall changes in matrix composition or architecture. However, this will require further functional analysis of whole ECM, which is ongoing.

PDI proteins have already been implicated in human disease and are said to have roles in haemostasis, infectious disease, lipid homeostasis, neurodegeneration, cancer and infertility[12-16]; we now know that it is also involved in bone disease (OI).

In this report, we demonstrate that Cole Carpenter syndrome is caused by a recurrent *P4HB* mutation with a very specific clinical and radiological phenotype and provide further clues to the underlying genotype. We have shown that possibly P4HB acts on collagen synthesis not by affecting the global secretion of procollagen type I from cells but in maintaining a functional ECM.

ACKNOWLEDGEMENTS

We thank this family for their participation in this report; Professor David J Amor, University of Melbourne for providing us with input regarding his patient and Dr Adam Benham, University of Durham for critical review of the manuscript. We would also like to thank

Matthew Parker and Emilie Jarratt at Sheffield Diagnostic Genetics Service for their assistance with the exome sequencing.

This research was supported by The Sheffield Children's Hospital Charity (TCHC) grant number CA15001 and a postgraduate scholarship from the University of Bristol to JM.

Author Roles: All authors contributed to preparation and critical review of manuscript; MB: Study design; writing up manuscript, recruitment of patient; phenotyping; RP, NJB, MZM: patient phenotyping; ACO: radiology input; RCP: exome sequencing; BEW: EM studies; JM, DJS: functional studies on hpf.

COMPETING INTERESTS

No competing interest to declare.

REFERENCES

1. Cole DE and Carpenter TO. Bone fragility, craniosynostosis, ocular proptosis, hydrocephalus, and distinctive facial features: a newly recognized type of osteogenesis imperfecta. J Pediatr 1987.110:76-80.

2. Amor DJ, Savarirayan R, Schneider AS, Bankier A. New case of Cole-Carpenter syndrome. Am J Med Genet. 2000 Jun 5;92(4):273-7.

3. Balasubramanian M, Pollitt RC, Chandler KE, Mughal MZ, Parker MJ, Dalton A,Arundel P, Offiah AC, Bishop NJ. . CRTAP mutation in a patient with Cole-Carpenter syndrome. Am J Med Genet A. 2015 Mar;167A(3):587-91. doi: 10.1002/ajmg.a.36916.

4. Rauch F, Fahiminiya S, Majewski J, Carrot-Zhang J, Boudko S, Glorieux F, Mort JS, Bächinger HP, Moffatt P. Cole-Carpenter syndrome is caused by a heterozygous missense mutation in P4HB. Am J Hum Genet. 2015 Mar 5;96(3):425-31. doi: 10.1016/j.ajhg.2014.12.027.

5. Garbes L, Kim K, Rieß A, Hoyer-Kuhn H, Beleggia F, Bevot A, Kim MJ, Huh YH, Kweon HS, Savarirayan R, Amor D, Kakadia PM, Lindig T, Kagan KO, Becker J, Boyadjiev SA, Wollnik B, Semler O, Bohlander SK, Kim J, Netzer C. Mutations in SEC24D, encoding a component of the COPII machinery, cause a syndromic form of osteogenesis imperfecta. Am J Hum Genet. 2015 Mar 5;96(3):432-9. doi: 10.1016/j.ajhg.2015.01.002.severity assessment.

6. McCaughey J, Miller VJ, Stevenson NL, Brown AK, Budnik A, Heesom KJ, Alibhai D, Stephens DJ. TFG Promotes Organization of Transitional ER and Efficient Collagen Secretion. Cell Rep. 2016;15:1648–1659.

7. Benham AM. The protein disulfide isomerase family: key players in health and disease. Antioxid. Redox Signal. 2012; 16, 781–789.

8. Hatahet F, and Ruddock LW. Protein disulfide isomerase: a critical evaluation of its function in disulfide bond formation. Antioxid. Redox Signal. 2009; 11, 2807–2850.

9. LaMantia M, Miura T, Tachikawa H, Kaplan HA, Lennarz WJ, Mizunaga T. Glycosylation site binding protein and protein disulfide isomerase are identical and essential for cell viability in yeast. Proc. Natl. Acad. Sci. USA 1991; 88, 4453–4457.

10. Kosuri P, Alegre-Cebollada J, Feng J, Kaplan A, Inglés-Prieto A, Badilla CL, Stockwell BR, Sanchez-Ruiz JM, Holmgren A, Fernández JM. Protein folding drives disulfide formation. Cell. 2012 Nov 9;151(4):794-806. doi: 10.1016/j.cell.2012.09.036.

11. Ishikawa Y and Ba¨chinger HP. A molecular ensemble in the rER for procollagen maturation. Biochim. Biophys. Acta 2013; 1833, 2479–2491.

12. Gruber CW, Cemazar M, Heras B, Martin JL, Craik DJ. Protein disulfide isomerase: the structure of oxidative folding. Trends Biochem Sci. 2006 Aug;31(8):455-64.

13. Pajunen L, Jones TA, Goddard A, Sheer D, Solomon E, Pihlajaniemi T, Kivirikko KI. Regional assignment of the human gene coding for a multifunctional polypeptide (P4HB) acting as the beta-subunit of prolyl 4-hydroxylase and the enzyme protein disulfide isomerase to 17q25. Cytogenet Cell Genet. 1991;56(3-4):165-8.

14. Soares Moretti AI, Martins Laurindo FR. Protein disulfide isomerases: Redox connections in and out of the endoplasmic reticulum. Arch Biochem Biophys. 2017 Mar 1;617:106-119. doi: 10.1016/j.abb.2016.11.007.

15. van Anken E, Braakman I. Endoplasmic reticulum stress and the making of a professional secretory cell. Crit Rev Biochem Mol Biol. 2005 Sep-Oct;40(5):269-83.

16. Wilkinson B, and Gilbert HF. Protein disulfide isomerase. Biochim. Biophys. Acta 2004; 1699, 35–44.

FIGURE LEGENDS

Figure 1a-d: Photographs of patient (frontal and profile) demonstrating frontal bossing, blueish grey sclerae, flat nasal bridge, prominent veins; limb deformities aged 6-months (Figure 1a-c) and aged 3 years (Figure 1d).

Figure 2: Selected radiographs from a skeletal survey (aged 6 months)

2a: AP right forearm 2b: AP left forearm 2c: AP right leg

There is generalised reduction in bone density with relative flaring of the metaphyses. There are slightly angulated and displaced transverse fractures at the junction of metaphyses and diaphyses of all imaged bones except the humeri. Note the irregular metaphyseal sclerosis at the fracture sites, but also of distal humerus and proximal radius and ulna, where there are no fractures. Symmetrical metadiaphyseal fractures of this nature are uncommon in OI.

There is a further minimally displaced fracture of the shaft of the left radius (arrow).

2d: Lateral spine: There are multiple vertebral compression fractures.

Figure 2e: AP and lateral right femur (aged 10 months)

Osteopenia, flared metaphyses and an acute metadiaphyseal junction fracture in a slightly more proximal position than the previous fracture. As in Figure 2a, note the irregular sclerosis around the healing fracture. Sclerosis (but no fractures) is also seen around the proximal tibial and fibular metaphyses.

Figure 2f: Lateral right forearm, lateral right leg (aged 31 months)

There is significant bowing deformity of the forearm and leg bones. The bones are dense, presumably due to bisphosphonate therapy (note bisphosphonate lines at distal radial and ulnar metaphyses and dense periphery of the tarsal bones). There are healing fractures of the right mid radial and distal humeral shafts.

Figure 3: Sequencing electropherograms demonstrating a heterozygous c.1178A>G mutation predicted to result in a p.(Tyr393Cys) amino acid change was identified in the *P4HB* gene (NM_000918.3) (Figure 3b) and normal trace in mother (Figure 3a).

Figure 4a-b: 4a: Electron microscopy demonstrating scattered small collagen fibrils within a bundle of unremarkable fibrous collagen. Original magnification x20,000; 4b: Proteoglycan

fibres wrapping around collagen fibrils. Original magnification x12, 000 (indicated by arrows).

Figure 5a-d: Immunofluorescence and subsequent quantification of extracellular collagen I of control and patient-derived skin fibroblasts after 30 minutes (A-B) and 24 hours (C-D) of ascorbic acid-2-phosphate. 5.a-c: Maximum projection of Z-Stacks consisting of 24 slices with $\Delta z = 0.08$ µm. Scale bar indicates 50 µm. 5.c/d: Quantification of 5.a and 5.c for mid-intensity values (16-62% or 40-159; empty shapes) and high-intensity values (63-100% or 160-255; filled shapes) for control (circles) and patient (squares). The mean is displayed in gray. Error bars show the standard deviation.

Figure 5e: Western Blot showing COL1a1 levels in control and patient primary fibroblasts. Lanes show fractions of medium (M) and lysate (L) of control and patient cells incubated with (+), or without ascorbate acid (-) for 24h. Expected band size for COL1a1 monomer 140kDa, dimer with COL1a2 270kDa, trimer 400kDa.

Table1: Comparison of clinical, radiological and molecular diagnosis in patients reported with CCS with patient reported here.

Table 1:

	This patient	Cole & Carpenter 1987 Patient 1	Cole & Carpenter 1987 Patient 2	Amor 2000	Balasubramanian 2015	Garbes 2015 Patient 1	Garbes 2015	Garbes 2015
Age	3y	4y	18m	30m	12y	7y	Fetus 1	Fetus 2
Sex	F	M	M	F	F	M	F	F
Ethnicity	White	White	White	White	Asian	German	German	German
Consanguinity	No	No	No	No	Yes	No	No	No
Molecular diagnosis	*P4HB* c.1178A>G, p.Tyr393Cys	*P4HB* c.1178A>G, p.Tyr393Cys (Rauch et al., 2015)	*P4HB* c.1178A>G, p.Tyr393Cys (Rauch et al., 2015)	NK	*CRTAP* c.118G>T,p.Glu40*	*SEC24D* c.613C>T, p.Gln205*; c.3044C>T,p.Ser1015Phe	*SEC24D* c.2933A>C, p.Gln978Pro (mat); c.3044C>T,p.Ser1015Phe (pat)	*SEC24D* c.2933A>C, p.Gln978Pro (mat); c.3044C>T,p.Ser1015Phe (pat)
Prenatal Fractures	-	-	-	-	-	+	++	++
Postnatal Fractures	++	++	++	+	++	+	NA	NA
Craniosynostosis	-	+	-	+	+	+	NA	NA
Vertebral Fractures/ Scoliosis	++	++	++	+	++	+	NA	NA
MCF	+	+	+	-	-	-	-	NA
Wormian bones	+	+	-	+	+	+	NA	NA
BP Therapy	+	+?	+?	+	+	+	NA	NA
Ocular proptosis	+	+	+	+	+	+	NA	NA
Blue sclerae	+	+	+	+	+	+	NA	NA
Macrocephaly	+	+	+	+	+	+	NA	NA
Hydrocephalus	-	+	+	-	-	+	NA	NA
DI	-	+	-	+	+	-	NA	NA
Intelligence	N	N	N	N	N	N	NA	NA

MCF: metaphyseal compression fractures; NA: Not available/ applicable; NK: Not known yet; ?+: Increase in BMD, no clinical response

Figure 1a-d

a

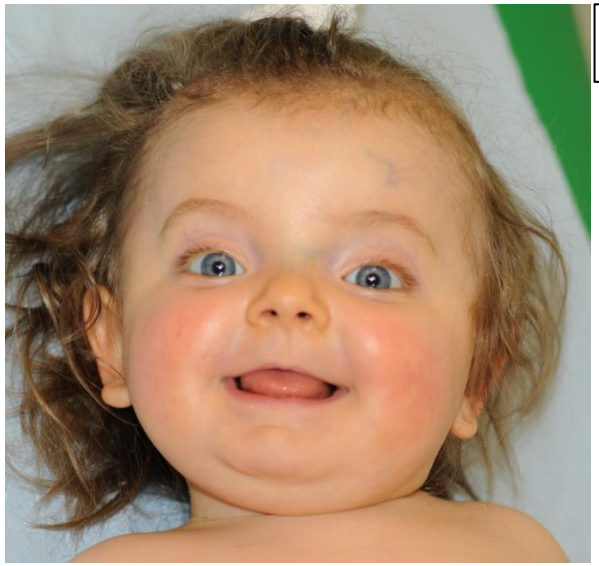

6-months

b

c

d

3-years

Figure 2a-d

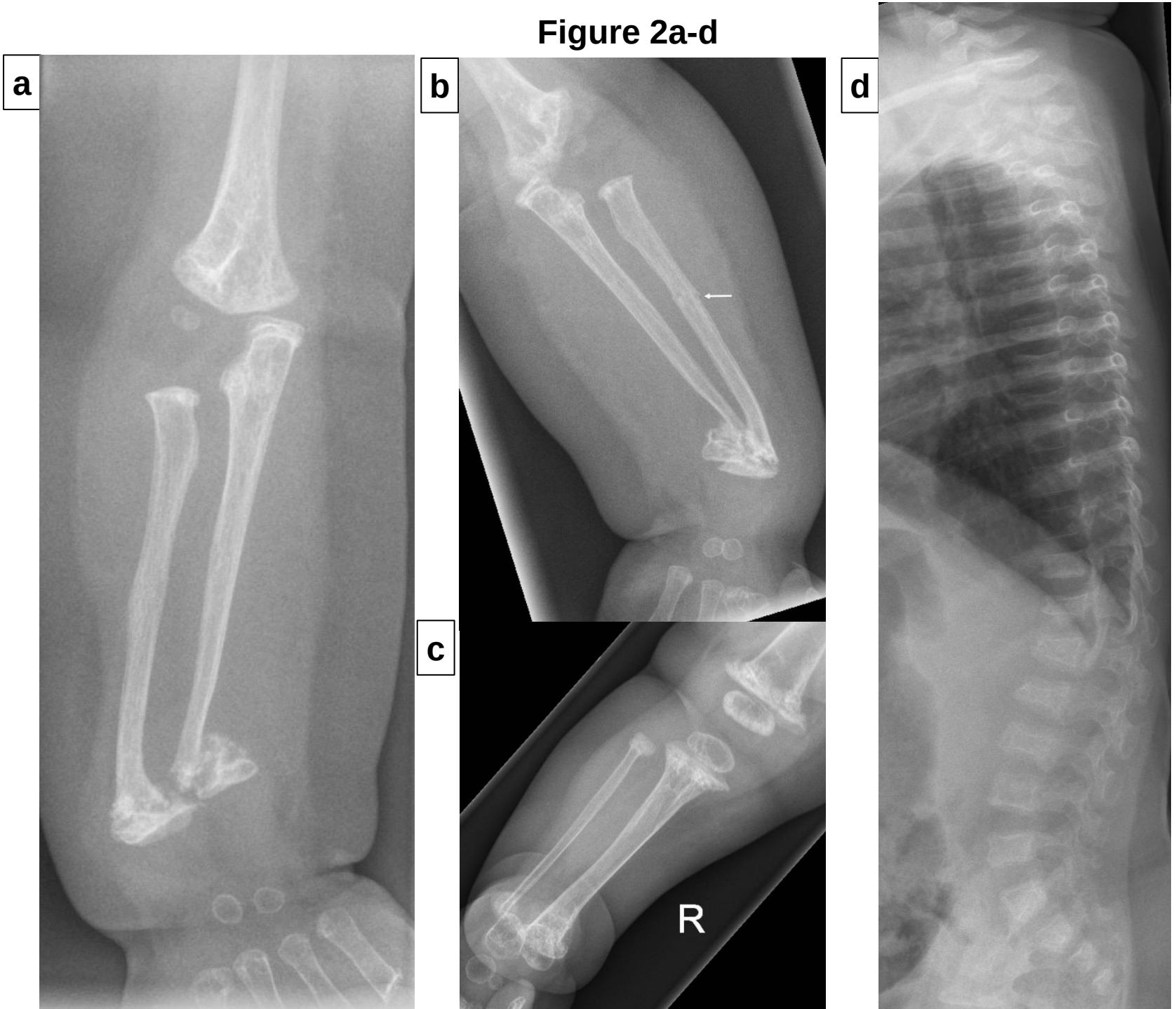

Figure 2e-f

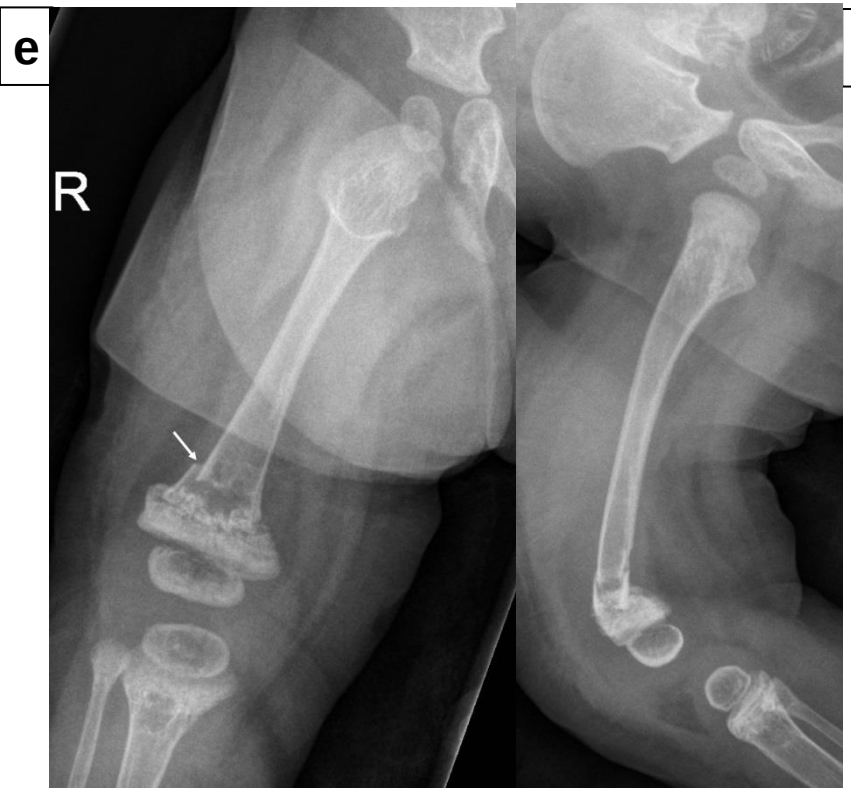

Figure 3

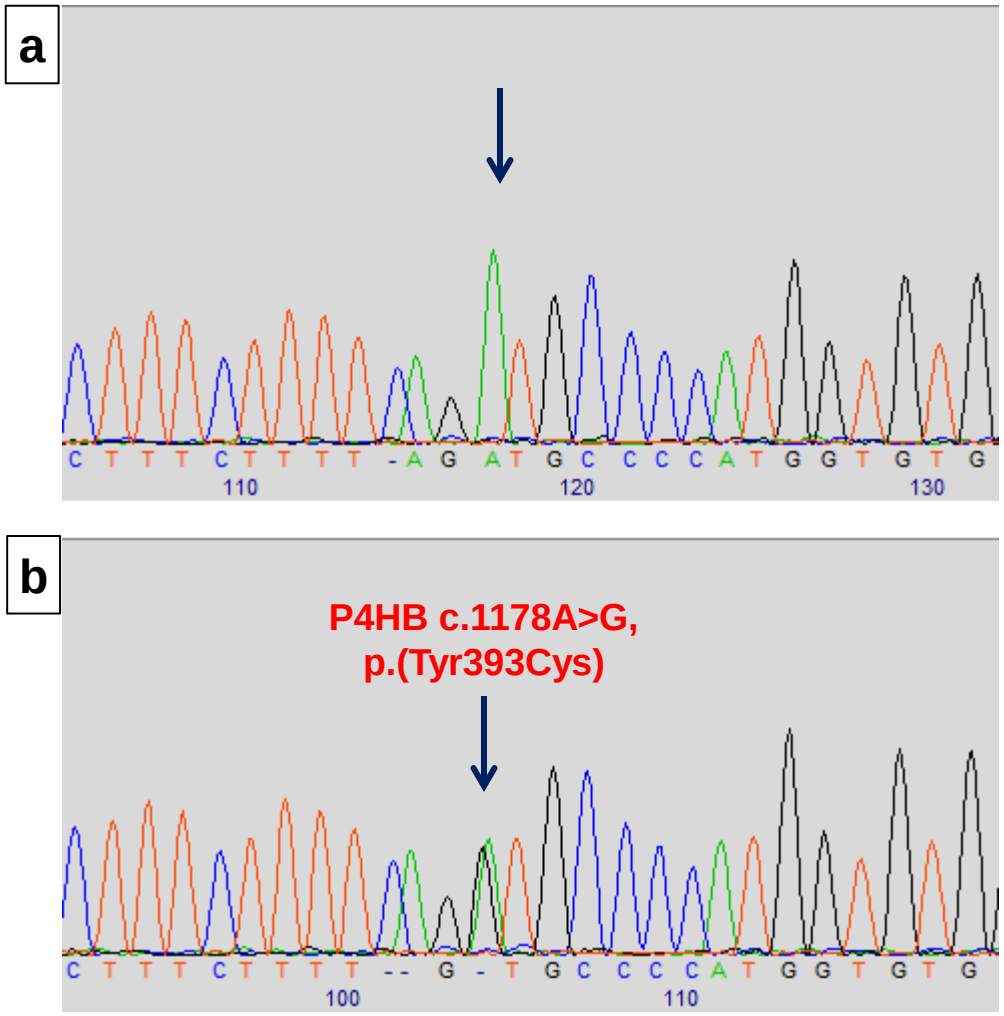
a
C T T T C T T T T - A G A T G C C C C A T G G T G T G
110
120
130
b
P4HB c.1178A>G,
p.(Tyr393Cys)
C T T T C T T T T - - G - T G C C C C A T G G T G T G
100
110

Figure 4

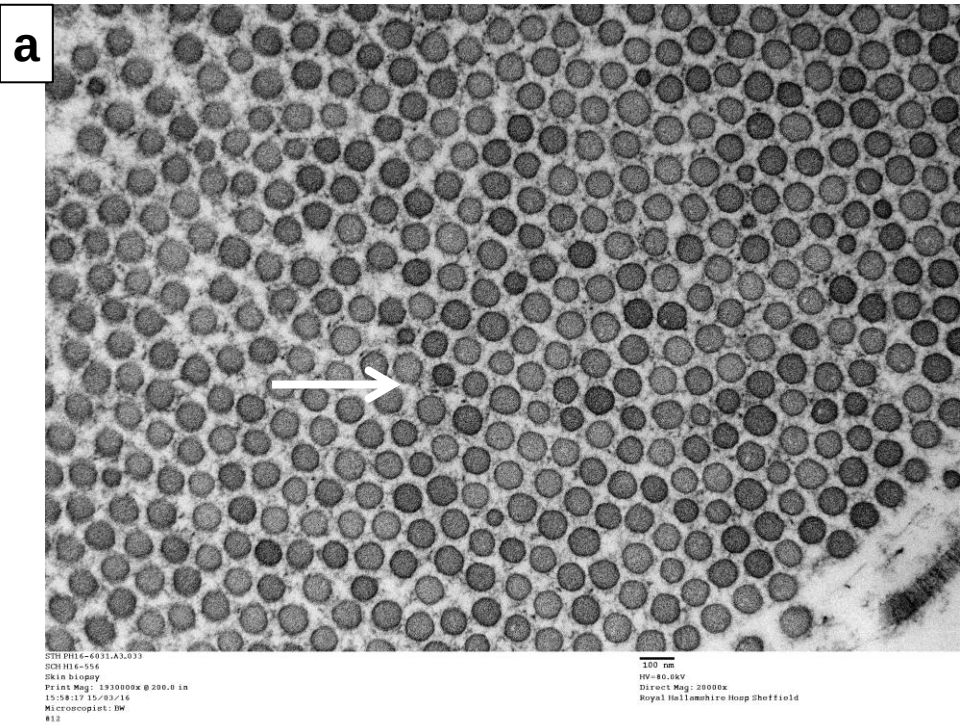
a
STH PH16-6031.A3.033
SCH H16-556
Skin biopsy
Print Mag: 1930000x @ 200.0 in
15:58:17 15/03/16
Microscopist: BW
812
100 nm
HV=80.0kV
Direct Mag: 28000x
Royal Hallamshire Hosp Sheffield

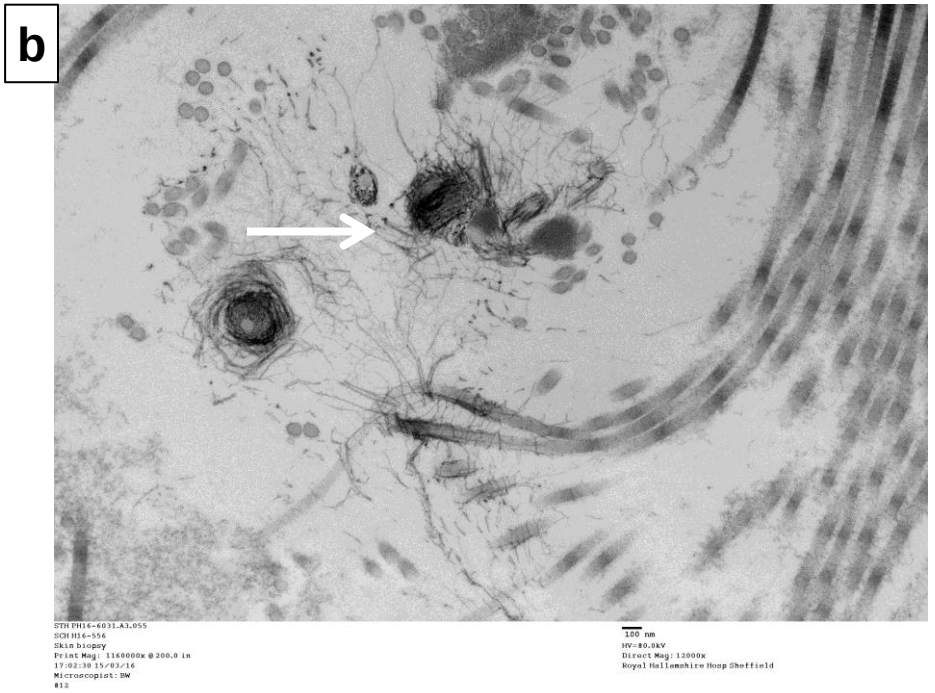
b
STH PH16-6031.A3.055
SCH H16-556
Skin biopsy
Print Mag: 1160000x @ 200.0 in
17:02:38 15/03/16
Microscopist: BW
812
100 nm
HV=80.0kV
Direct Mag: 12000x
Royal Hallamshire Hosp Sheffield

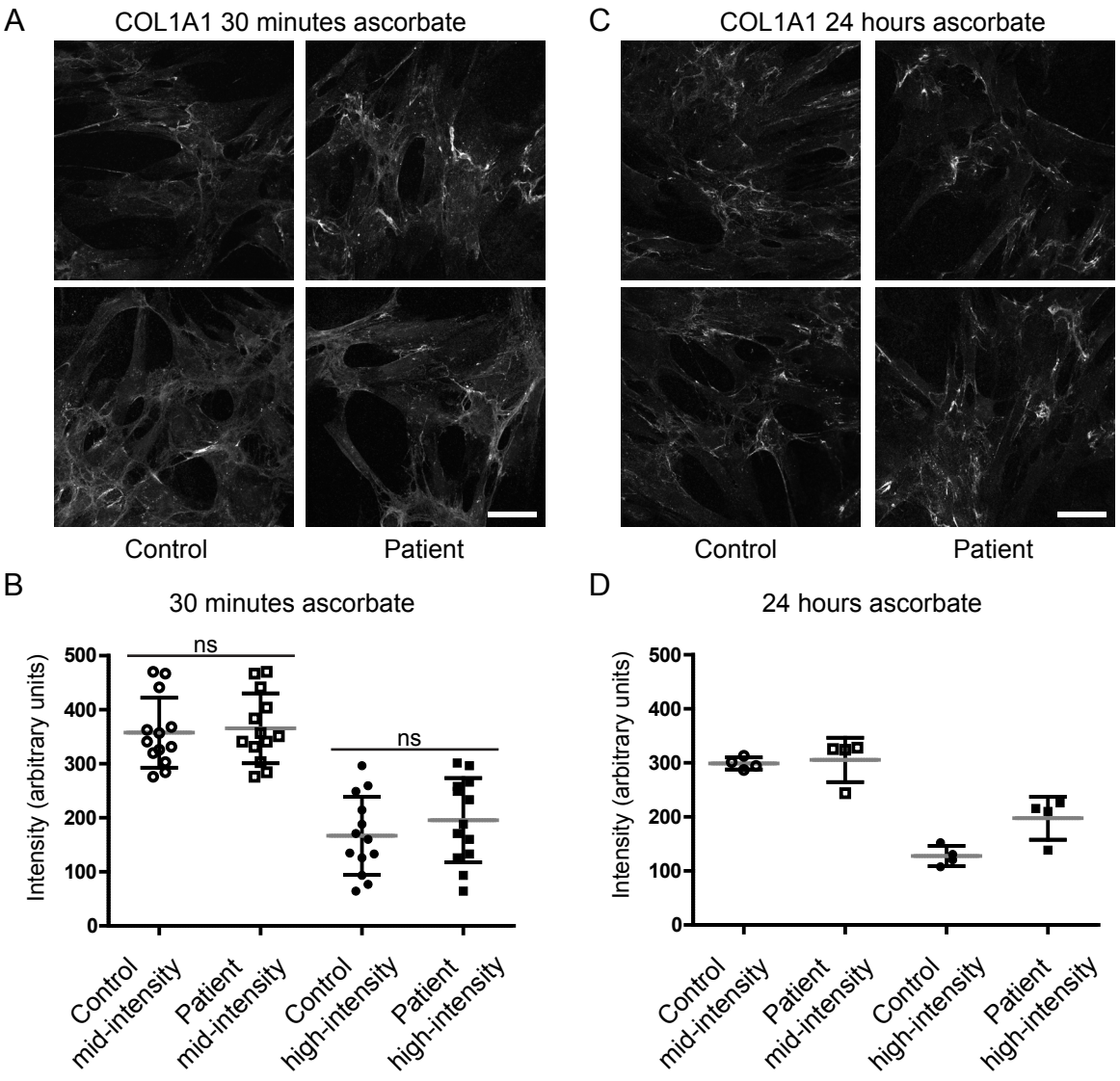
A
COL1A1 30 minutes ascorbate
C
COL1A1 24 hours ascorbate
Control
Patient
Control
Patient
B
30 minutes ascorbate
Intensity (arbitrary units)
500
400
300
200
100
0
ns
ns
Control mid-intensity
Patient mid-intensity
Control high-intensity
Patient high-intensity
D
24 hours ascorbate
Intensity (arbitrary units)
500
400
300
200
100
0
Control mid-intensity
Patient mid-intensity
Control high-intensity
Patient high-intensity

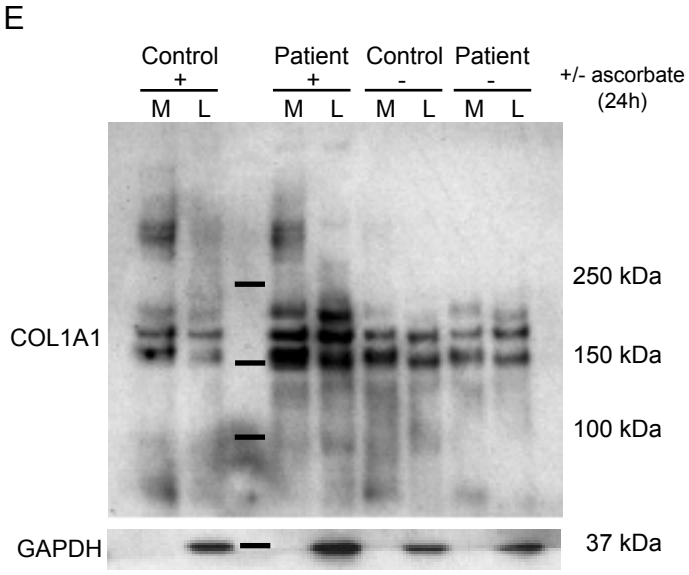
E
Control
+
Patient
+
Control
-
Patient
-
M L M L M L M L
+/- ascorbate
(24h)
COL1A1
250 kDa
150 kDa
100 kDa
GAPDH
37 kDa